IOSR Journal of Mechanical and Civil Engineering (IOSR-JMCE)
e-ISSN: 2278-1684,p-ISSN: 2320-334X, Volume 12, Issue 4 Ver. I (Jul. - Aug. 2015), PP 17-28
www.iosrjournals.org

Impact of changing the position of the tool point on the moving platform on the dynamic performance of a 3RRR planar parallel manipulator

Roshdy Foaad Abo-Shanab
Department of Mechanical Engineering, Faculty of Engineering / Kafrelsheikh University, Egypt.

Abstract: *In this paper, the impact of changing the location of the tool point, on the moving platform, on the dynamics of a planar parallel manipulator is investigated. Lagrange-d'Alembert formulation is used to develop the dynamic model of the present manipulator. To evaluate the dynamic performance of the parallel manipulator, the input efforts and energy consumptions are calculated for the manipulator when the end-effector is positioned at different locations on the moving platform and executing given desired trajectories. The manipulator's dimensions and parameters are kept the same during the optimization process and only the position of the tool-point on the moving platform is changed. The dynamic performance of the manipulator is then evaluated and optimized. It is shown that locating the end-effector of the manipulator at an optimum position reduces the generalized forces required to drive the manipulator. It also reduces the energy consumption of the manipulator.*

Keywords - *Dynamics, energy consumption, Lagrange-d'Alembert, optimization, parallel manipulators, trajectory.*

I. Introduction

In recent years, many studies have focused on parallel manipulators. Since their end-effector, moving platform, is sustained by several kinematic chains, parallel manipulators can achieve better structural and dynamic properties with less structural mass. Some of the advantages offered by parallel manipulators, when properly designed, include a high load-to-weight ratio, high stiffness, and positioning accuracy. However, parallel manipulators are difficult to design, since the relationships between design parameters and the workspace, and behavior of the manipulator throughout the workspace, are not intuitive by any means [1]. In addition, the performances of parallel manipulators are very sensitive to their dimensioning. Therefore, a thorough analysis of the kinematic and dynamic behavior of the parallel manipulators should be developed for optimal design of these machines [2]. Parallel manipulators also are more energy efficient than serial manipulators. Li and Gary [3] showed that over a range of conditions, the average energy usage of the parallel manipulator was determined to be 26% of the serial manipulator's. In this respect, Pellicciari et al. [4] showed a slight improve in the energy consumption on favor of parallel manipulators in pick and place industrial robots application.

In a previous article [5], the author studied the kinematic behavior of a 3RRR planar manipulator as the location of the tool point, on the moving platform, changes. It was shown that changing the location of the end-effector on the moving platform greatly affects the kinematics of a parallel manipulator as the area of the workspace changes as well as other performance indices such as the global conditioning index. It was recommended that the location of the end-effector on the moving platform should be considered while optimizing the performance of a parallel manipulator. The dynamic performance of the parallel manipulator has not been studied in the article.

Dynamical analysis of parallel manipulators is complicated by the existence of the multiple closed-loop chains. Several approaches have been proposed including the Newton-Euler formulation [6-8], the Lagrangian formulation [9-12], and the Lagrange-D'Alembert formulation [13-16]. For the Newton-Euler formulation, one first carries out a detailed force and torque analysis of each rigid link with some physical knowledge such as Newton's third law, and then apply Newton's second law and Euler's equation to each of the rigid links to obtain a set of second order ordinary differential equations in the position and angular representation of each rigid link. Finally together with the kinematic constraints, the set of equations can be simplified or solved, till the desired form of dynamics equation is obtained. The Lagrangian approach is a more efficient than Newton-Euler method as it eliminates the unwanted reaction forces and moments at the outset. However, because of the numerous constraints imposed by the closed loops of parallel manipulator, deriving explicit equations of motion in terms of a set of independent generalized coordinates becomes a prohibitive task. Therefore, the Lagrangian equations are written in terms of a set of redundant coordinates. The formulation then requires a set of constraint equations derived from the kinematics of the manipulator. Final equations of motion are derived and arranged in

two sets. One contains Lagrange multipliers as the only unknown, and the other contains the generalized forces contributed by the actuator as the traditional unknowns [17]. Lagrange-d'Alembert formulation allows deriving the equations of motion without explicitly solving for the instantaneous constraint forces present in the system. This proceeds by projecting the motion of the system into the feasible directions and ignoring the forces of constraints directions. By doing so, a more concise description of the dynamics can be obtained [18].

Yiu et al. [19] reviewed various methods used in deriving the dynamic equations for parallel manipulators. They proposed to cut the links instead of cutting joints to obtain the tree system, so that all the joints torques, including joint friction, can be incorporated in the dynamic equations.

Khan et al. [20] developed a modular and recursive formulation for the inverse dynamics of parallel architectures based on the concept of decoupled natural orthogonal complement. They applied the developed method to derive the dynamic equations of a 3RRR planar parallel manipulator. They cut the moving platform into three parts to form three open chains, to be able to apply torques at the joints, and to include the joint friction.

Wu et al. [21] investigated and compared the dynamics of the planar 3-DOF 4-RRR, 3-RRR and 2-RRR parallel manipulators. The 2-RRR parallel manipulator has only two limbs and one of these limbs has two active (actuated) joints whereas the 4-RRR planar manipulator has a redundant actuator. They showed that the sum of the absolute values of driving torques of the 2-RRR manipulator has the largest range. They concluded that the 2-RRR parallel manipulator has the worst dynamic performance among the three planar 3-DOF parallel mechanisms and, in some regions of the workspace, the dynamic performance of the 4-RRR manipulator is better than that of the 3-RRR one.

Ruiz et al. [22] studied the impact of kinematic and actuation redundancy on the energy efficiency of planar parallel kinematic machines. They concluded that optimal energy efficient trajectories are dependent on the manipulator architecture and redundant parallel manipulators are more energy efficient than non-redundant manipulators.

Generally, it is considered that, given a desired trajectory, the robot that has the lowest input efforts and lowest energy consumption along the trajectory has the best performance.

The objective of this text is to show the effects of changing the location of the tool point, on the moving platform, on the dynamics and energy efficiency of planar parallel manipulators. To the best of the author's knowledge, none of the previous work has discussed this problem.

The manipulator geometry is presented in Section 2. In Section 3, the dynamic model of the studied manipulator is developed using Lagrange-d'Alembert formulation. Two case studies are used to evaluate the dynamic performance and energy consumption of the manipulator and discussion of the simulation results are presented in Section 4. In Section 5, conclusions are described.

II. Manipulator Geometry

The manipulator considered in this work is a *3RRR* planar parallel mechanism. A schematic diagram of the manipulator is shown in Figure 1. The manipulator consists of a moving equilateral triangular platform of length h connected to a fixed equilateral triangular base of length d by three limbs. Each limb consists of two links; the first link is connected to the ground by means of a revolute joint identified by the letter B_i and is actuated by a rotary actuator. The three actuators, one for each limb, control the three degrees of freedom of the moving platform (x, y, and φ). Two coordinate systems are defined to describe the motion of the moving platform. The first coordinate system is attached to the fixed base (with origin O and axes x and y) and is called the reference frame while the second coordinate system is attached to the moving frame (with origin O' and axes x' and y').

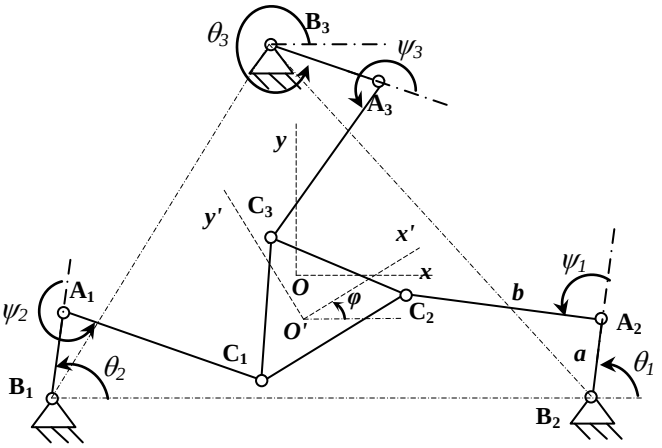

Fig. 1. A 3-RRR parallel manipulator

In the present work, we change the location of the manipulator end-effector, the position of O' in Figure 2, within the area of the moving triangle $C_1\ C_2\ C_3$ to find the optimal position with respect to the dynamic performance of the manipulator. The pose of the end-effector is expressed relative to the reference frame by the position vector $Z = [x\ y\ \varphi]$. The input angles $\Theta = [\theta_1\ \theta_2\ \theta_3]$ is represented by the angular positions of the revolute actuators measured from the x-axis of the reference coordinate system. The inverse

kinematics and Jacobian analysis of the manipulator were presented by the author in a previous article [16] and are presented in the appendices for the convenience of the reader.

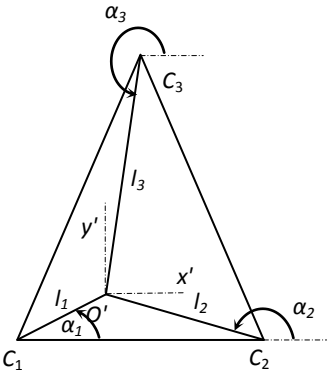

Fig. 2. Definition of the moving plate parameters

III. Dynamic Analysis

A parallel manipulator can be considered as a mechanical system with configuration $q \in R^n$ subject to a set of holonomic constrains, for the present manipulator, $q = [\theta_1\theta_2\theta_3\, x\, y\, \varphi]^T$. A constraint is said to holonomic if it restricts the motion of the system to a smooth hypersurface in the, unconstrained, configuration space Q [18]. Holonomic constraints can be represented locally as algebraic constraints on the configuration space,

$$h_i(q) = 0, \quad i = 1,..,k \tag{1}$$

where k is the number of linearly independent constraints. Each h_i is a mapping from the configuration space Q to $\mathbb{R}$ restricts the motion of the system. Let $L(q, \dot{q})$ represents the Lagrangian for the unconstrained system. We assume that the constraints are everywhere smooth and linearly independent and that the forces of constraint do no work on the system. The equations of motion are formed by considering the constraint forces as an additional force which affects the motion of the system. Hence, the dynamics can be written in vector form as

$$\frac{d}{dt}\frac{\partial L}{\partial \dot{q}} - \frac{\partial L}{\partial q} = A^T\lambda + \tau \tag{2}$$

$$\text{where } A = \frac{\partial h}{\partial q} = \begin{bmatrix} \frac{\partial h_1}{\partial q_1} & \cdots & \frac{\partial h_1}{\partial q_n} \\ \vdots & \ddots & \vdots \\ \frac{\partial h_k}{\partial q_n} & \cdots & \frac{\partial h_k}{\partial q_n} \end{bmatrix} \tag{3}$$

The columns of A^T form non-normalized bases for the constraint forces and $\lambda \in \mathbb{R}^k$ are called Lagrange multipliers and gives the relative magnitude of the forces of constraints. τ represents nonconservative and externally applied forces.

At a given configuration $q \in R^n$, the instantaneous set of directions in which the system is allowed to move is given by the null space of the constraint matrix, $A(q)$. Let the vector $\delta q \in R^n$, which satisfies $A(q) \cdot \delta q = 0$, a virtual displacement. Then $\delta W = \tau \cdot \delta q$ is called the virtual work due to a force τ acting along a virtual displacement δq. D'Alembert's principle states that the forces of constraint do no virtual work. Hence,

$$(A^T(q)\lambda) \cdot \delta q = 0 \tag{4}$$

To eliminate the constraint forces from Equation (2), the equations of motion is projected onto the linear subspace generated by the null space of $A(q)$.

$$\left(\frac{d}{dt}\frac{\partial L}{\partial \dot{q}} - \frac{\partial L}{\partial q} - \tau\right) \cdot \delta q = 0 \tag{5}$$

where $\delta q \in R^n$ satisfies the constraints

$$A(q) \cdot \delta q = 0$$

Rearrange the matrix $A(q)$ to take the following form

$$A(q) = [A_\Theta(q)\, A_z(q)]$$

where $A_\Theta(q) = \frac{\partial h}{\partial \Theta}$, $A_z(q) = \frac{\partial h}{\partial Z}$, $\Theta = [\theta_1\theta_2\theta_3]^T$, and $Z = [x\, y\, \varphi]^T$.

Let $\tau = [\tau_\Theta;\, F]$ where $\tau_\Theta = [\tau_1;\, \tau_2;\, \tau_3]$ is a column vector of the actuating torques and $F = \left[F_x;\, F_y;\, \tau_\varphi\right]$ is a column vector of the external forces and torques. Then, Equation (5) can be written as follows:

$$\left(\frac{d}{dt}\frac{\partial L}{\partial \dot{q}} - \frac{\partial L}{\partial q} - \tau\right) \cdot \delta q = \begin{bmatrix} \frac{d}{dt}\frac{\partial L}{\partial \dot{\Theta}} - \frac{\partial L}{\partial \Theta} - \tau_\Theta \\ \frac{d}{dt}\frac{\partial L}{\partial \dot{Z}} - \frac{\partial L}{\partial Z} - F \end{bmatrix} \cdot \begin{bmatrix} \delta\Theta \\ \delta Z \end{bmatrix} = 0$$

$$\left(\frac{d}{dt}\frac{\partial L}{\partial \dot{\Theta}} - \frac{\partial L}{\partial \Theta} - \tau_\Theta\right) \cdot \delta\Theta + \left(\frac{d}{dt}\frac{\partial L}{\partial \dot{Z}} - \frac{\partial L}{\partial Z} - F\right) \cdot \delta Z = 0$$

$$\left(\frac{d}{dt}\frac{\partial L}{\partial \dot{\Theta}} - \frac{\partial L}{\partial \Theta} - \tau_\Theta\right) \cdot \delta\Theta + \left(\frac{d}{dt}\frac{\partial L}{\partial \dot{Z}} - \frac{\partial L}{\partial Z} - F\right) \cdot (-[A_Z(q)]^{-1}A_\Theta(q)\delta\Theta) = 0$$

Since $\delta\Theta$ is free, then

$$\left(\frac{d}{dt}\frac{\partial L}{\partial \dot{\theta}} - \frac{\partial L}{\partial \theta} - \tau_\theta\right) + (-[A_\theta(q)]^T[A_Z(q)]^{-T})\left(\frac{d}{dt}\frac{\partial L}{\partial \dot{Z}} - \frac{\partial L}{\partial Z} - F\right) = 0$$

Then the actuator torques can be written as follows:

$$\tau_\Theta = \frac{d}{dt}\frac{\partial L}{\partial \dot{\theta}} - \frac{\partial L}{\partial \theta} + (-[A_\theta(q)]^T[A_Z(q)]^{-T})\left(\frac{d}{dt}\frac{\partial L}{\partial \dot{Z}} - \frac{\partial L}{\partial Z} - F\right) \quad (6)$$

Equation (6) represents the dynamic model of a general parallel manipulator that is subject to holonomic constraints and calculates directly the actuator torques without explicitly calculating the Lagrange multipliers.

For the present manipulator, different terms of Equation (6) can be determined as follows. First, the constraint equations of the manipulator, see Figure 1, can be written as:

$$h_i = [x - x_{Bi} - a\cos\theta_i - l_i\cos(\alpha_i + \varphi)]^2 + [y - y_{Bi} - a\sin\theta_i - l_i\sin(\alpha_i + \varphi)]^2 - b^2 = 0 \quad (7)$$

Then,

$$A_\theta(q) = \begin{bmatrix} h_{11} & 0 & 0 \\ 0 & h_{22} & 0 \\ 0 & 0 & h_{33} \end{bmatrix} \quad (8)$$

and

$$A_Z(q) = \begin{bmatrix} h_{1x} & h_{1y} & h_{1\varphi} \\ h_{2x} & h_{2y} & h_{2\varphi} \\ h_{3x} & h_{3y} & h_{3\varphi} \end{bmatrix} \quad (9)$$

where

$$h_{ij} = \frac{\partial h_i}{\partial \theta_j} = 0 \qquad \text{for } i \neq j$$

$$h_{ii} = \frac{\partial h_i}{\partial \theta_i} = 2a\,[(x - x_{Bi})\sin\theta_i - (y - y_{Bi})\cos\theta_i + l_i\sin(\alpha_i + \varphi - \theta_i)]$$

$$h_{ix} = \frac{\partial h_i}{\partial x} = 2(x - x_{Bi} - a\cos\theta_i - l_i\cos(\alpha_i + \varphi))$$

$$h_{iy} = \frac{\partial h_i}{\partial y} = 2(y - y_{Bi} - a\sin\theta_i - l_i\sin(\alpha_i + \varphi))$$

$$h_{i\varphi} = \frac{\partial h_i}{\partial \varphi} = 2\,l_i\,[(x - x_{Bi})\sin(\alpha_i + \varphi) - (y - y_{Bi})\cos(\alpha_i + \varphi) - a\sin(\alpha_i + \varphi - \theta_i)]$$

Since $A(q)\cdot\delta q = 0$, then

$$\dot{\theta} = -[A_\theta(q)]^{-1}A_z(q)\,\dot{z} \quad (10)$$

Let $A_{\theta z}(q) = -[A_\theta(q)]^{-1}A_Z(q)$

$$A_{\theta z}(q) = -\begin{bmatrix} h_{11} & 0 & 0 \\ 0 & h_{22} & 0 \\ 0 & 0 & h_{33} \end{bmatrix}^{-1}\begin{bmatrix} h_{1x} & h_{1y} & h_{1\varphi} \\ h_{2x} & h_{2y} & h_{2\varphi} \\ h_{3x} & h_{3y} & h_{3\varphi} \end{bmatrix}$$

$$A_{\theta z}(q) = -\begin{bmatrix} \frac{h_{1x}}{h_{11}} & \frac{h_{1y}}{h_{11}} & \frac{h_{1\varphi}}{h_{11}} \\ \frac{h_{2x}}{h_{22}} & \frac{h_{2y}}{h_{22}} & \frac{h_{2\varphi}}{h_{22}} \\ \frac{h_{3x}}{h_{33}} & \frac{h_{3y}}{h_{33}} & \frac{h_{3\varphi}}{h_{33}} \end{bmatrix} \quad (11)$$

Let $\dot{A}_{\theta z}(q) = \frac{d}{dt}[A_{\theta z}(q)]$, the elements of $\dot{A}_{\theta z}(q)$ can be calculated as follows:

$$\frac{d}{dt}\left(\frac{h_{ix}}{h_{ii}}\right) = \frac{\dot{h}_{ix}h_{ii} - h_{ix}\dot{h}_{ii}}{h_{ii}^2}$$

$$\frac{d}{dt}\left(\frac{h_{iy}}{h_{ii}}\right) = \frac{\dot{h}_{iy}h_{ii} - h_{iy}\dot{h}_{ii}}{h_{ii}^2}$$

$$\frac{d}{dt}\left(\frac{h_{i\varphi}}{h_{ii}}\right) = \frac{\dot{h}_{i\varphi}h_{ii} - h_{i\varphi}\dot{h}_{ii}}{h_{ii}^2}$$

where

$$\dot{h}_{ix} = \dot{x} + a\sin\theta_i\,\dot{\theta}_i + l_i\sin(\alpha_i+\varphi)\,\dot{\varphi}$$

$$\dot{h}_{iy} = \dot{y} - a\cos\theta_i\,\dot{\theta}_i - l_i\cos(\alpha_i+\varphi)\,\dot{\varphi}$$

$$\dot{h}_{i\varphi} = l_i\left[\dot{x}\,\sin(\alpha_i+\varphi) + (x-x_{Bi})\,\cos(\alpha_i+\varphi)\dot{\varphi} - \dot{y}\cos(\alpha_i+\varphi) + (y-y_{Bi})\,\sin(\alpha_i+\varphi)\,\dot{\varphi} - a\cos(\alpha_i+\varphi-\theta_i)\left(\dot{\varphi}-\dot{\theta}_i\right)\right]$$

$$\dot{h}_{ii} = a\left[(x-x_{Bi})\cos\theta_i\,\dot{\theta}_i + \dot{x}\sin\theta_i + (y-y_{Bi})\,\sin\theta_i\,\dot{\theta}_i - \dot{y}\,\cos\theta_i + l_i\cos(\alpha_i+\varphi-\theta_i)\left(\dot{\varphi}-\dot{\theta}_i\right)\right]$$

If the motion of the tool-point of the parallel kinematic machine is defined in the Cartesian coordinates, the time derivatives of the joint variables can be calculated as follows.

$$\dot{\theta} = A_{\theta z}(q)\dot{Z} \tag{12}$$

$$\ddot{\theta} = A_{\theta z}(q)\ddot{Z} + \dot{A}_{\theta z}(q)\dot{Z} \tag{13}$$

Next, the Lagrangian function of the manipulator is calculated. The manipulator is planar moves in a horizontal plane, therefore, potential energy is zero and the Lagrangian function is simply equals to the total kinetic energy of the manipulator. The kinetic energy of the manipulator can be divided into three parts; the kinetic energy of the first link in each limb, the second link in each limb, and the moving platform. First, the kinetic energy, K_{a_i}, of the first link in each limb (Link $B_i A_i$), note that the limbs are identical :

$$K_{a_i} = \frac{1}{2}m_a v_{a_i}^2 + \frac{1}{2}I_a\dot{\theta}_i^2 \tag{14}$$

$v_{a_i} = \frac{1}{2}a\,\dot{\theta}_i$ is the velocity of the center of mass of link $B_i A_i$, m_a is the mass of link $B_i A_i$, $I_a = \frac{1}{12}m_a a^2$ is the mass moment of inertia of link $B_i A_i$ about an axis passing through its center of mass and parallel to *z*-axis, and a is the length of link $B_i A_i$. Then

$$K_{a_i} = \frac{1}{6}m_a a^2\theta_i^2 \tag{15}$$

The kinetic energy of the second link, K_{b_i}, in each limb (Link $A_i\ C_i$):

$$K_{b_i} = \frac{1}{2}m_b v_{b_i}^2 + \frac{1}{2}I_b\left(\dot{\theta}_i + \dot{\psi}_i\right)^2 \tag{16}$$

where v_{bi} is the velocity of the center of mass of link $A_i C_i$, m_b is the mass of link $A_i C_i$, and $I_b = \frac{1}{12}m_b b^2$ is the mass moment of inertia of link $A_i C_i$ about an axis passing through its center of mass and parallel to *z*-axis. The kinetic energy of the second link of each limb is derived as a function of $x, y, \varphi, \theta_1, \theta_2$, and θ_3 and their time derivatives and ψ_1, ψ_2, ψ_3 and their time derivatives are eliminated.

$$K_{b_i} = \frac{1}{6}m_b\left[\dot{x}^2 + \dot{y}^2 + a^2\dot{\theta}_i^2 + l_i^2\dot{\varphi}_i^2 - \dot{\theta}_i(\dot{x}\sin\theta_i - \dot{y}\cos\theta_i) + 2l_i\dot{\varphi}(\dot{x}\sin(\alpha_i+\varphi) - \dot{y}\cos(\alpha_i+\varphi)) - 2al_i\dot{\varphi}\dot{\theta}_i\cos(\alpha_i+\varphi-\theta_i)\right] \tag{17}$$

Finally, the kinetic energy of the moving plate K_p:

$$K_p = \frac{1}{2}m_p v_p^2 + \frac{1}{2}I_p\dot{\varphi}^2$$

where v_p is the velocity of the origin of the moving coordinate system that attached to the moving plate and I_p is the mass moment of inertia of the moving platform.

From (15), (16) and (17), the total kinetic energy of the manipulator is

$$L = \frac{1}{2}\left(m_b + m_p\right)\dot{x}^2 + \frac{1}{2}\left(m_b + m_p\right)\dot{y}^2 + \frac{1}{2}\left[\frac{1}{3}(l_1^2 + l_2^2 + l_3^2)m_b + I_p\right]\dot{\varphi}^2 + \frac{1}{6}(m_a + m_b)\,a^2\sum_{i=1}^{3}\dot{\theta}_i^2 + \left[\frac{1}{3}\,m_b\dot{\varphi}\sum_{i=1}^{3}l_i\sin(\alpha_i+\varphi) - \frac{1}{6}a\,m_b\sum_{i=1}^{3}\sin\theta_i\,\dot{\theta}_i\right]\dot{x} + \left[-\frac{1}{3}\,m_b\dot{\varphi}\sum_{i=1}^{3}l_i\cos(\alpha_i+\varphi) + \frac{1}{6}a\,m_b\sum_{i=1}^{3}\cos\theta_i\,\dot{\theta}_i\right]\dot{y} - \frac{1}{6}a\,m_b\dot{\varphi}\sum_{i=1}^{3}l_i\cos(\alpha_i+\varphi-\theta_i)\dot{\theta}_i \tag{18}$$

Taking the derivatives of the Lagrangian function (19) with respect to the six generalized coordinates, we get

$$\frac{\partial L}{\partial x} = 0, \tag{19}$$

$$\frac{\partial L}{\partial y} = 0, \tag{20}$$

and

$$\frac{\partial L}{\partial \varphi} = \frac{1}{3}\, m_b \left(\sum_{i=1}^{3} l_i \cos(\alpha_i + \varphi)\, \dot{x} + l_i \sin(\alpha_i + \varphi)\, \dot{y}\right) \dot{\varphi} + \frac{1}{6} a\, m_b \dot{\varphi} \sum_{i=1}^{3} l_i \sin(\alpha_i + \varphi - \theta_i) \dot{\theta}_i \qquad (21)$$

$$\frac{\partial L}{\partial \theta_i} = -\frac{1}{6} a\, m_b (\dot{x} \cos\theta_i + \dot{y} \sin\theta_i) \dot{\theta}_i - \frac{1}{6} a\, l_i\, m_b \sin(\alpha_i + \varphi - \theta_i) \dot{\theta}_i \dot{\varphi}, \; i = 1, 2, \text{and } 3. \qquad (22)$$

$$\frac{\partial L}{\partial \varphi} = \frac{1}{3}\, m_b \left(\sum_{i=1}^{3} l_i \cos(\alpha_i + \varphi)\, \dot{x} + l_i \sin(\alpha_i + \varphi)\, \dot{y}\right) \dot{\varphi} + \frac{1}{6} a\, m_b \dot{\varphi} \sum_{i=1}^{3} l_i \sin(\alpha_i + \varphi - \theta_i) \dot{\theta}_i \qquad (23)$$

$$\frac{d}{dt}\left(\frac{\partial L}{\partial \dot{x}}\right) = \left(m_b + m_p\right) \ddot{x} + \frac{1}{3}\, m_b \ddot{\varphi} \sum_{i=1}^{3} l_i \sin(\alpha_i + \varphi) - \frac{1}{6} a\, m_b \sum_{i=1}^{3} \sin\theta_i\, \ddot{\theta}_i + \frac{1}{3}\, m_b \dot{\varphi}^2 \sum_{i=1}^{3} l_i \cos(\alpha_i + \varphi) - \frac{1}{6} a\, m_b \sum_{i=1}^{3} \cos\theta_i\, \dot{\theta}_i^2 \qquad (24)$$

$$\frac{d}{dt}\left(\frac{\partial L}{\partial \dot{y}}\right) = \left(m_b + m_p\right) \ddot{y} - \frac{1}{3}\, m_b \left[\sum_{i=1}^{3} l_i \cos(\alpha_i + \varphi)\, \ddot{\varphi} - \sum_{i=1}^{3} l_i \sin(\alpha_i + \varphi) \dot{\varphi}^2\right] + \frac{1}{6} a\, m_b \sum_{i=1}^{3} \cos\theta_i\, \ddot{\theta}_i - \frac{1}{6} a\, m_b \sum_{i=1}^{3} \sin\theta_i\, \dot{\theta}_i^2 \qquad (25)$$

$$\frac{d}{dt}\left(\frac{\partial L}{\partial \dot{\varphi}}\right) = \left(\frac{1}{3}(l_1^2 + l_2^2 + l_3^2) m_b + I_p\right) \ddot{\varphi} + \frac{1}{3}\, m_b \left(\sum_{i=1}^{3} l_i \sin(\alpha_i + \varphi)\, \ddot{x} - l_i \cos(\alpha_i + \varphi)\, \ddot{y}\right) - \frac{1}{6} a\, m_b \sum_{i=1}^{3} \cos(\alpha_i + \varphi - \theta_i) \ddot{\theta}_i + \frac{1}{3} m_b \dot{\varphi} \left(\sum_{i=1}^{3} l_i \cos(\alpha_i + \varphi)\, \dot{x} + l_i \sin(\alpha_i + \varphi)\, \dot{y}\right) + \frac{1}{6} a\, m_b \sum_{i=1}^{3} \sin(\alpha_i + \varphi - \theta_i) \left(\dot{\varphi} - \dot{\theta}_i\right) \dot{\theta}_i \qquad (26)$$

$$\frac{d}{dt}\left(\frac{\partial L}{\partial \dot{\theta}_i}\right) = \frac{1}{3}(m_a + m_b)\, a^2 \ddot{\theta}_i - \frac{1}{6} a\, m_b (\ddot{x} \sin\theta_i - \ddot{y} \cos\theta_i + l_i \cos(\alpha_i + \varphi - \theta_i) \ddot{\varphi}) - \frac{1}{6} a\, m_b \left(\dot{x}\, \dot{\theta}_i \cos\theta_i + \dot{y}\, \dot{\theta}_i \sin\theta_i - l_i \sin(\alpha_i + \varphi - \theta_i)(\dot{\varphi} - \dot{\theta}_i) \dot{\varphi}\right), \; i = 1, 2, \text{and } 3. \qquad (27)$$

Equations (8) to (9) and (19) to (27) are substituted in Equation (6) to obtain the driving torques. Meanwhile, the energy consumption of the parallel manipulator can be expressed as follows [9]:

$$E = \int_{t_o}^{t_f} \left(\sum_{i=1}^{3} |\tau_i \theta_i|\right) dt \qquad (28)$$

where t_o and t_f are the start time and end time, respectively of the motion of the manipulator.

IV. Simulation Results

The developed schemes are applied to the present manipulator, shown in Figure 1. The coordinates of the points of connection of the manipulator with the fixed base are: $B_1(-300, -173.2)$ mm, $B_2(300, -173.2)$ mm and $B_3(0, 346.4)$ mm. The following numerical values are used for the different manipulator dimensions: $a = 150$ mm, $b = 337.5\ mm$, $h = 250$ mm. The author showed in a previous article [23] that these dimensions give the maximum reachable workspace of the manipulator. Inertia moments and masses of different links of the manipulator are taken as follows: $m_a = 2$ kg, $m_b = 4.5$ kg, $m_p = 3$ kg, and $I_p = 0.03$ kg.m^2. The external forces, $F = [F_x\ F_y\ \tau_\varphi]$, are assumed to be constant during the motion with the following values: $F_x = 20\ N$, $F_y = 10\ N$, and $\tau_\varphi = 0$ N.m.

To evaluate the dynamic performance of the parallel manipulator, the input efforts and energy consumed are calculated for the manipulator when the end-effector is positioned at different locations on the moving platform and executes given desired trajectories. Figure 3 shows the different locations of the tool point on the moving platform, these locations are chosen based on the similarity of the platform (equilateral triangle), other locations are expected to give similar results.

Two trajectories are assigned for the motion of the tool point. The first trajectory is a straight-line path the tool point moves from the initial location at $Z = [40\ \ -100\ \ \pi/3]^T$, where x and y are in millimeters and φ is in radians, to the final position at $Z = [-40\ \ -100\ \ \pi/3]^T$ with cycloidal motion:

$$x = x_o - l * [t/T - 1/2\pi * \sin(2\pi t/T)] \qquad (29)$$

Where y and φ are constants during the path and $l = 80$ mm, is the total distance traveled by the tool point during the task.

The second trajectory is to move the tool point on a circular path of radius $R = 40$ mm and a center at $(x_o = -10\ mm, y_o = -100\ mm,)$, starts from the initial location at $Z = [40\ \ -100\ \ \pi/3]^T$. The equations of the motion trajectory are:

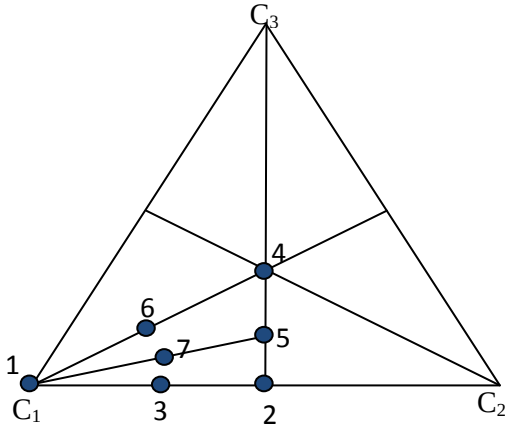

Fig. 3. Different locations for the tool point on the moving platform.

$$Z = \begin{bmatrix} x_o + R\cos 2\pi t/T \\ y_o + R\sin 2\pi t/T \\ \pi/3 \end{bmatrix} \quad (30)$$

where $T = 4$ s, is the total motion time in both cases. For the second trajectory, the tool point makes a complete circle in 4 seconds. The orientation of the moving platform is kept constant during the motion at $\varphi = \pi/3$ and the integration time is chosen to be $\Delta t = 1$ ms. Figures 4 and 5 show the trajectories of the moving platform during the two cases.

A MATLAB program is developed to calculate the actuator torques for both trajectories considering the tool point at different locations as shown in Fig. 3. The program also calculates the energy required to execute the manipulator motion. The results show that the input efforts are the lowest when the tool point is located at Position 1. Fig. 5 and Fig. 6 show the required torques to drive the manipulator through a straight-line path while the tool point is at Position 4 and Position 1, respectively. Fig. 7 shows the sum of torques when the tool point is located at Position 1, 4, and 5. Figs. 9 to 11 show similar results when the tool point is moving on a circular path. The two sets of results, moving on a straight-line path and on a circular path, give the same indication about the dynamic performance of the manipulator, Position 1 give the lowest input effort to drive the manipulator through the desired trajectories.

The optimization toolbox *fminimax* of MATLAB, which applies Quasi-Newton algorithm, is used to find the location of the tool point on the moving platform that optimizes the energy consumption during the execution of trajectory in the two cases. For both cases, it is found that Position 1gives the minimum energy consumption. The results are verified using a MATLAB program. The energy consumption of the manipulator during the execution of the tasks when the tool point is positioned at different locations is calculated. As seen in Fig. 12, Position 1 gives the lowest energy consumption for both trajectories.

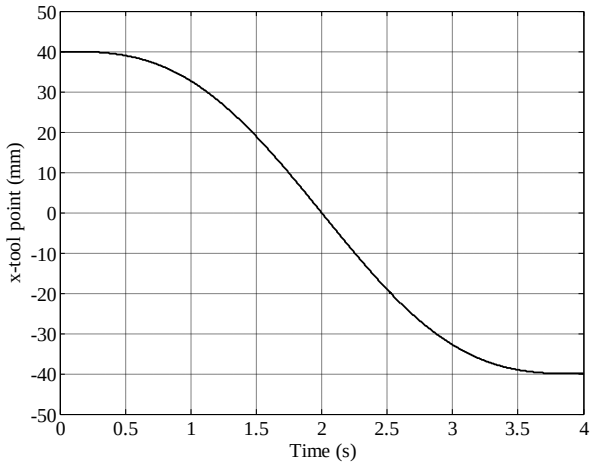

Fig. 4. *x*- Coordinate of the tool point during the first case.

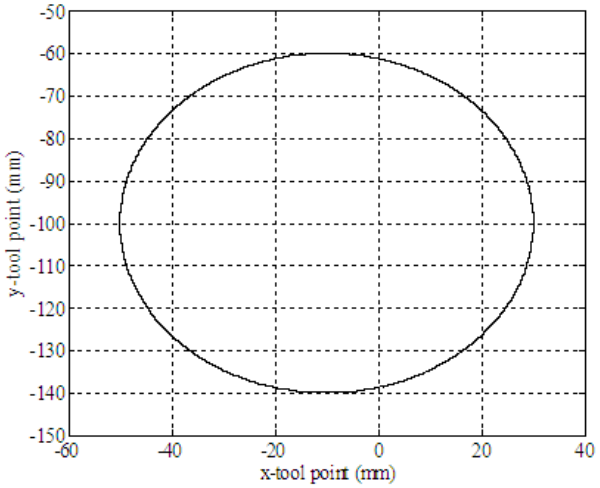

Fig. 5. Tool point Trajectory during the second case.

V. Conclusion

The present work investigates the effects of changing the position of the end-effector, on the moving platform, on the dynamic performance of a 3-RRR planar parallel manipulator. The dynamic equations of the parallel manipulator were developed using Lagrange d'Alembert method. The dynamic performance of the manipulator was then optimized as the location of the tool point on the moving platform changes. All the dimensions and parameters of the manipulator are kept the same during the optimization process. To the best of the author knowledge, none of the previous research had addressed this problem. It is shown that precisely locating the suitable tool point position on the moving platform reduces the input efforts and the energy consumption. For the present manipulator, the reductions of the energy consumption were 23.4% and 18.67% for the first and second cases, respectively.

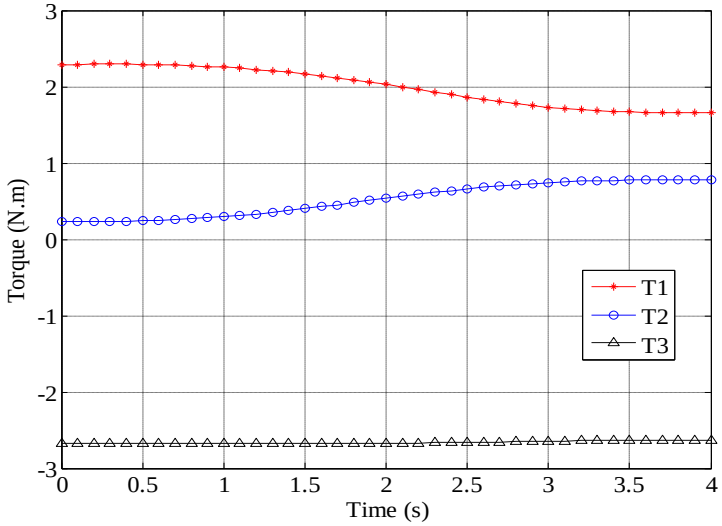

Fig. 6. Driving torque for the straight line path, tool point at position 4.

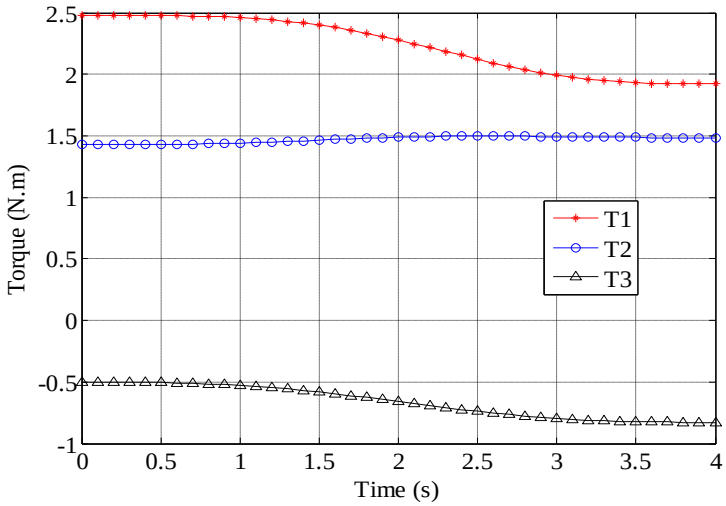

Fig. 7. Driving torque for the straight line path, tool point at position 1.

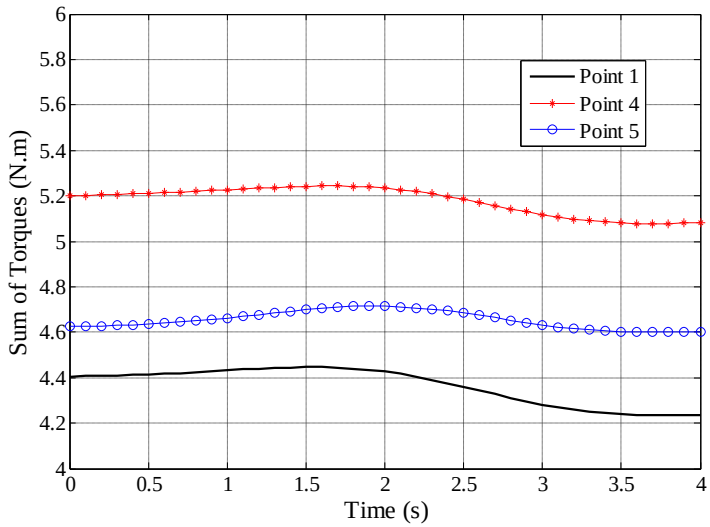

Fig. 8. Sum of the absolute values of the driving torque for the straight line path, tool point at different positions.

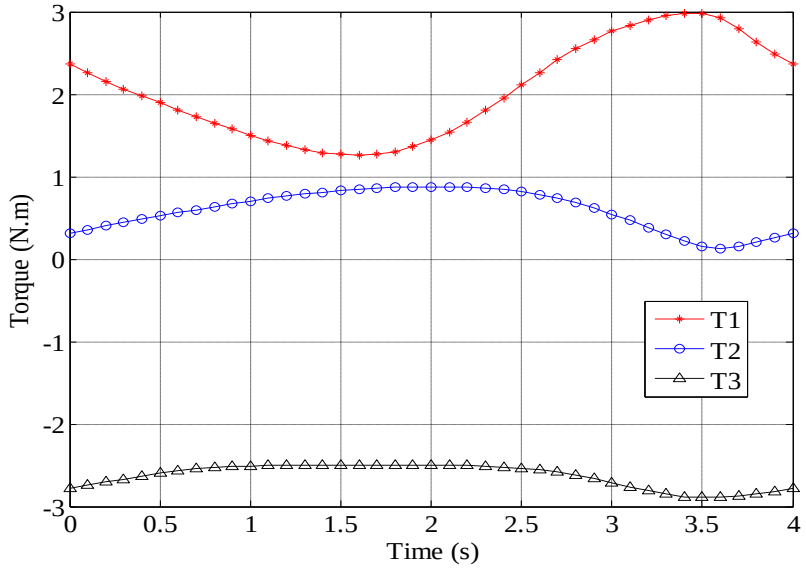

Fig. 9. Driving torque for the circular line path, tool point at position 4.

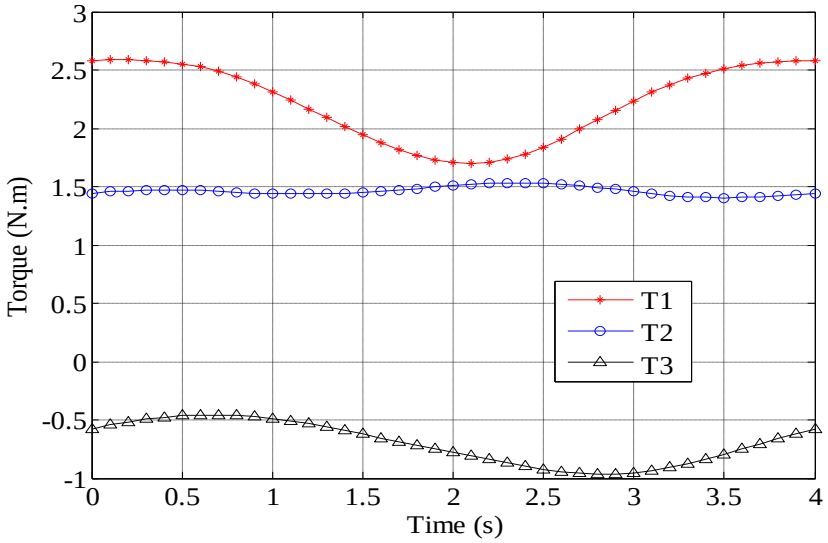

Fig. 10. Driving torque for the circular line path, tool point at position 1.

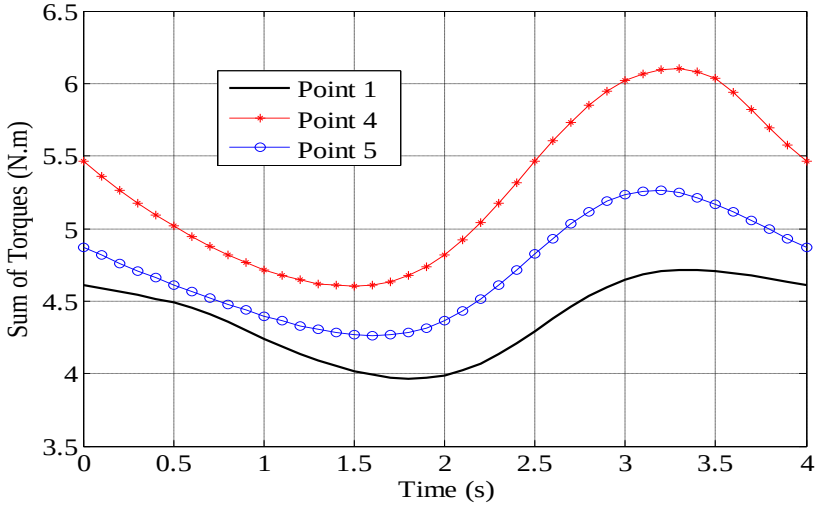

Fig. 11. Sum of the absolute values of the driving torque for the circular line path, tool point at different positions.

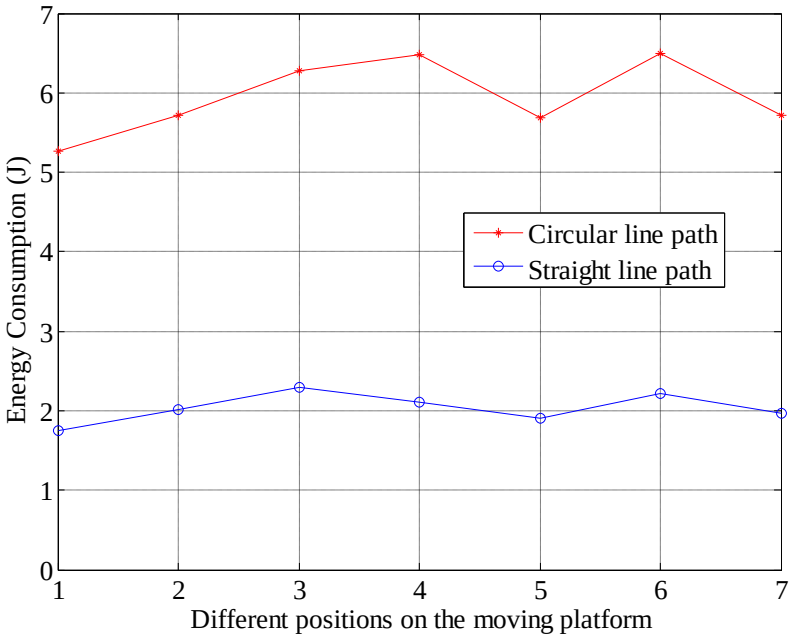

Fig. 12. Energy consumption during the straight line path and circular line path, tool point at different positions.

References

[1] C. Gosselin, L. Perrault, and C. Viallancourt, Simulation and computer-aided kinematic design of three-degree-of-freedom spherical parallel manipulator, Journal of Robotic Systems, 12, 1995, 857 – 869.

[2] J. P. Merlet, Jacobian, manipulability, condition number, and accuracy of parallel robots, ASME J. Mech. Des. 128, 2005, 199-206.

[3] Y. Li and M.B. Gary, Are Parallel Manipulators More Energy Efficient? Proceedings of 2001 IEEE International Symposium on computational Intelligence in Robotics and Automation, Banff, Alberta, Canada, 2001, 41-46.

[4] M. Pellicciari, G. Berselli, F. Leali, and A. Vergnano, "A method for reducing the energy consumption of pick and place industrial robots," Mechatronics, 23(3), 2013, 326-334.

[5] R.F. Abo-Shanab, Effect of changing the position of tool point on the moving platform on the kinematics of a 3RRR Planar Parallel Manipulator, Applied Mechanics and Materials Vols. 541-542, 2014, 792-797.

[6] W.Q.D. Do and D.C.H. Yang, Inverse Dynamic analysis and simulation of a platform type of a robot, Journal of Robotic Systems, 5(3), 1988, 209-227.

[7] P. Guglielmetti and R. Longchamp, A closed form inverse dynamic model of the delta parallel robot," Proceedings of the 1994 International Federation of Automatic Control Conference on Robot Control, 1994, 30-44.

[8] K.Y. Tsai and D. Kohli, Modified Newton-Euler computational scheme for dynamic analysis and simulation of parallel manipulators with application to configuration based on R-L actuators, Proceedings of the 1990 ASME Design Engineering Technical Conferences, Vol. 24, Boston, Massachusetts, 1990, 111-117.

[9] S. Liu, Z. Zhu, Z. Sun, and G. Cao, Kinematics and dynamic analysis of a three-degree of freedom parallel manipulator, Journal of Central South University, Vol. 21,2014, 2660-2666.

[10] Y.Nakamura, and M. Ghodoussi, "Dynamics Computation of Closed-Link Robot Mechanisms with Nonredundant and Redundant Actuators,"IEEE Trans. Robot. Automat., vol.5(3), pp. 294 – 302, 1989.

[11] Y.Naramura, and Katsu Yamane, "Dynamics Computation of Structure-Varying Kinematic Chains and Its Application to Human Figures," IEEE Trans. Robot. Automat., 16(2), 2000, 124 – 134.

[12] F.C. Park, J. Choi, and S.R. Ploen, Symbolic Formulation of Closed Chain Dynamics in Independent Coordinates, Mechanism and Machine Theory, 1999, vol. 34, 731-751.

[13] A. Codourey and E. Burdet, A body oriented method for finding a linear form of the dynamic equation of fully parallel robots, Proceedings of 1997 IEEE International conference on Robotics and Automation, 1997, 1612-1618.

[14] L.W. Tsai, solving the inverse dynamics of parallel manipulators by the principle of virtual work, Proceedings of 1998 ASME Design Engineering Technical Conferences, DETC98/MECH-5865.

[15] J. Wang and C.M. Gosselin, Dynamic analysis of spatial four-degrees-of-freedom parallel manipulators, Proceedings of 1997 ASME Design Engineering Technical Conferences, DETC97/DAC-3759.

[16] H. Cheng, Y. Yiu, and Z. Li, Dynamics and control of redundantly actuated parallel manipulators, IEEE/ASME Transactions on Mechatronics, 8(4), 2003, 483-491.

[17] L.W. Tsai, Robot Analysis: the mechanics of serial and parallel manipulators, (John Wiley and Sons, USA 1999).

[18] R. Murray, Z.X. Li, and S. Sastry, A Mathematical Introduction to Robotic Manipulation, (CRC Press, 1994).

[19] Y.K. Yiu, H. Cheng, Z.H. Xiong, G.F. Liu, and Z.X. Li, "On Dynamics of Parallel Manipulators," Proceedings of 20001 IEEE international Conference on Robotics and Automation, 2001, 3766-3771.

[20] W. Khan, V. Krovi, S. Saha, and J. Angeles, Recursive Kinematics and Inverse Dynamics for a 3R Parallel Manipulator, Journal of Dynamic Systems, Measurements, and Control, Vol. 127, 2005, 529-536.

[21] J. Wu, J. Wang, and Z. You, "A comparison study on the dynamics of planar 3-DOF 4RRR, 3RRR, and 2-RRR parallel manipulator," Robotics and Computer-Integrated Manufacturing, vol. 27, 2011, 150-156.

[22] A.G. Ruiz, J.V.C. Fontes, and M.M. da Silva, The impact of the Kinematics and Actuation Redundancy on the Energy Consumption of Planar Parallel Kinematic Machines, Proceedings of the XVII International Symposium on Dynamic Problems of Mechanics, DIN-2015-0033, 2015.

[23] R.F. Abo-Shanab, Optimization of the Workspace of a 3R Planar Parallel Manipulator, Proceedings of the 2nd International Conference on Mechanical and Electronics Engineering (ICMEE 2010), paper number M823, Vol. 2, 2010, 429-433.

Appendix A

Inverse Kinematics

From the geometry of the manipulator, shown in Figures 1 and 2, a vector loop equation can be written for each limb as

$$OO' = OB_i + B_iA_i + A_iC_i + C_iO' \quad \text{(A1)}$$

where $i = 1, 2, 3$. Expanding (1), we get

$$x = x_{Bi} + a\cos\theta_i + b\cos(\theta_i + \psi_i) + l_i\cos(\alpha_i + \varphi) \quad \text{(A2)}$$

$$y = y_{Bi} + a\sin\theta_i + b\sin(\theta_i + \psi_i) + l_i\sin(\alpha_i + \varphi) \quad \text{(A3)}$$

The definitions of the angles α_1, α_2, and α_3 are shown in Figure 2. Squaring (A2) and (A3) and summing the results, we get

$$b^2 = [x - x_{Bi} - a\cos\theta_i - l_i\cos(\alpha_i + \varphi)]^2 + [y - y_{Bi} - a\sin\theta_i - l_i\sin(\alpha_i + \varphi)]^2. \quad \text{(A4)}$$

Now, expanding (A4) and putting the result in the following form:

$$e_{i1}\sin\theta_i + e_{i2}\cos\theta_i + e_{i3} = 0, \quad \text{(A5)}$$

where

$$e_{i1} = 2a\rho_i\sin(\alpha_i + \varphi) + 2a(y_{Bi} - y) \quad \text{(A6)}$$

$$e_{i2} = 2a\rho_i\cos(\alpha_i + \varphi) + 2a(x_{Bi} - x) \quad \text{(A7)}$$

$$e_{i3} = x^2 + y^2 + a^2 + \rho_i^2 - b^2 - 2x\,x_{Bi} - 2y\,y_{Bi} + x_{Bi}^2 + y_{Bi}^2 + 2l_i\cos(\alpha_i + \varphi)(x_{Bi} - x) + 2l_i\sin(\alpha_i + \varphi)(y_{Bi} - y). \quad \text{(A8)}$$

Substitute the following trigonometric identities in (A5)

$$\sin\theta_i = \frac{2t_i}{1+t_i^2},\ \cos\theta_i = \frac{1-t_i^2}{1+t_i^2},\ \text{and}\ t_i = \tan\frac{\theta_1}{2}$$

we obtain

$$(e_{i3} - e_{i2})t_i^2 + 2e_{i1}t_i + (e_{i3} + e_{i2}) = 0, \quad \text{(A9)}$$

then

$$\theta_i = 2\tan^{-1}\frac{-e_{i1} \pm \sqrt{e_{i1}^2 + e_{i2}^2 - e_{i3}^2}}{e_{i3} - e_{i2}} \quad \text{(A10)}$$

Three cases could be found when solving (10). The first case when the solution gives two different real roots. This means that for each given moving platform location, there are two possible configurations for every limb. The second case, when it yields a double root, this means that this limb is in a fully stretched out or folded back configuration and is called the singular configuration. The third case, when the solution yields no real roots, the specified moving platform location is not reachable, i.e., this location is out of the manipulator workspace [17].

Appendix B

Jacobian Analysis of the Manipulator

In this section, the analytical development of the manipulator's Jacobian matrix is presented. For each limb, differentiating (A2) and (A3), we get:

$$\dot{x} = -a\sin\theta_i\,\dot{\theta}_i - b\sin(\theta_i + \psi_i)\left(\dot{\theta}_i + \dot{\psi}_i\right) - l_i\sin(\alpha_i + \varphi)\dot{\varphi}, \quad \text{(A11)}$$

$$\dot{y} = a\cos\theta_i\,\dot{\theta}_i + b\cos(\theta_i + \psi_i)\left(\dot{\theta}_i + \dot{\psi}_i\right) + l_i\cos(\alpha_i + \varphi)\dot{\varphi}. \quad \text{(A12)}$$

Solving (A11) and (A12) to eliminate $\dot{\psi}_i$, we get

$$\cos(\theta_i + \psi_i)\,\dot{x} + \sin(\theta_i + \psi_i)\,\dot{y} - l_i\sin[(\theta_i + \psi_i) - (\alpha_i + \varphi)]\dot{\varphi} = a\sin\psi_i\,\dot{\theta}_i. \quad \text{(A13)}$$

Equation (A13) is written in the matrix form as follows:

$$\boldsymbol{J_z\dot{Z} = J_\theta\dot{\Theta}}, \quad \text{(A14)}$$

where $\boldsymbol{J_z} = \begin{bmatrix} \cos\beta_1 & \sin\beta_1 & -l_1 \sin\left(\beta_1 - (\alpha_1 + \varphi)\right) \\ \cos\beta_2 & \sin\beta_2 & -l_2 \sin\left(\beta_2 - (\alpha_2 + \varphi)\right) \\ \cos\beta_3 & \sin\beta_3 & -l_3 \sin\left(\beta_3 - (\alpha_3 + \varphi)\right) \end{bmatrix}$, $\beta_i = \theta_i + \psi_i$, and

$$\boldsymbol{J_\theta} = \begin{bmatrix} a\sin\psi_1 & 0 & 0 \\ 0 & a\sin\psi_2 & 0 \\ 0 & 0 & a\sin\psi_3 \end{bmatrix}$$

In the above expression, $\boldsymbol{J_z}$ and $\boldsymbol{J_\theta}$ are two separate Jacobian matrices, these matrices can be combined to obtain a single matrix that establishes the inverse transformation between the input and output velocities:

$$\dot{\boldsymbol{\theta}} = \boldsymbol{J}\,\dot{\boldsymbol{Z}}, \tag{A15}$$

where $\boldsymbol{J} = \boldsymbol{J_\theta^{-1}} \boldsymbol{J_z}$ corresponding to the inverse Jacobian of a serial manipulator.